J|A|C|S
ARTICLES
Published on Web 03/30/2007

Synthesis and Exfoliation of $Co^{2+}-Fe^{3+}$ Layered Double Hydroxides: An Innovative Topochemical Approach

Renzhi Ma,* Zhaoping Liu, Kazunori Takada, Nobuo Iyi, Yoshio Bando, and Takayoshi Sasaki

Contribution from the Nanoscale Materials Center, National Institute for Materials Science, Namiki 1-1, Tsukuba, Ibaraki 305-0044, Japan

Received January 8, 2007; E-mail: ma.renzhi@nims.go.jp

Abstract: This paper describes a topochemical synthetic approach to $Co^{2+}-Fe^{3+}$ layered double hydroxides (LDHs). Micrometer-sized hexagonal platelets of brucite-like $Co_{2/3}Fe_{1/3}(OH)_2$ were first prepared by a homogeneous precipitation of an aqueous solution of divalent cobalt and ferrous ions through hexamethylenetetramine (HMT) hydrolysis under a nitrogen gas atmosphere. A subsequent oxidative intercalation process, by the action of iodine (I_2) in chloroform ($CHCl_3$), transformed the precursory brucite-like $Co^{2+}-Fe^{2+}$ hydroxides into hydrotalcite-like $Co^{2+}-Fe^{3+}$ LDHs, in which the oxidization of Fe^{2+} into Fe^{3+} induced positive charges to the octahedral hydroxyl layers while anions (I^-) were intercalated into the interlayer space. $Co^{2+}-Fe^{3+}$ LDHs inherited the high crystallinity and hexagonal platelet morphology from their brucite-like precursor due to the topotactic nature of the transformation, which was verified by abundant microscopic and spectroscopic characterizations. After a normal ion-exchange process, $Co^{2+}-Fe^{3+}$ LDHs accommodating perchlorate anions were exfoliated into unilamellar nanosheets in formamide by an ultrasonic treatment.

Introduction

Increasing attention has been paid to layered double hydroxides (LDHs), also known as hydrotalcite-like compounds and anionic clays, represented by a general formula of $[M^{2+}_{1-x}M^{3+}_x(OH)_2]^{x+}[A^{n-}_{x/n}]^{x-}\cdot mH_2O$ consisting of octahedral brucite-like host layers (M^{2+}/M^{3+}: divalent and trivalent metal cations; $x = 0.2-0.33$), charge-balancing anions (A^{n-}), and interlayer water molecules.[1] Theoretically, any combination of M^{2+} and M^{3+} cations, provided that their ionic radii do not significantly deviate from that of Mg^{2+}, is plausible in the LDH hydroxyl slabs.[2] This highly tunable intralayer composition, coupled with a wide possible choice of anionic moieties, affords a large variety of multifunctional LDH materials for potential applications as anion exchangers,[3] adsorbents,[4] catalysts,[5] solid-state nanoreactors and molecular sieves,[6] polymer composites, and bioactive materials.[7] Recently, extensive efforts have also been directed toward the delamination of LDHs into their unilamellar form, creating a new type of nanosheet with ultimate two-dimensional (2D) anisotropy and positive charge.[8-10] The unilamellar nanosheets of LDHs are ideal building blocks for functional assembly (multilayer films,[9e,10a,b] core/shells,[11] etc.) and might also exhibit unconventional physicochemical properties.[10b]

Although LDHs could be routinely obtained by a coprecipitation of constituting divalent and trivalent metallic species under slightly alkaline conditions, the resultant product was generally gel-like and of low crystalline quality.[12] Monodisperse and

(1) (a) Allmann, R. *Acta Crystallogr.* **1968**, *24B*, 972. (b) Miyata, S.; Okada, A. *Clays Clay Miner.* **1977**, *25*, 14. (c) Miyata, S. *Clays Clay Miner.* **1983**, *31*, 305. (d) Clearfield, A. *Chem. Rev.* **1988**, *88*, 125. (e) Braterman, P. S.; Xu, Z. P.; Yarberry, F. *Layered Double Hydroxides (LDHs), in Handbook of Layered Materials*; Auerbach, S. M., Carrado, K. A., Dutta, P. K., Eds.; Marcel Dekker, Inc.: New York, 2004.
(2) Bravo-Suárez, J. J.; Páez-Mozo, E. A.; Oyama, S. T. *Quim. Nova* **2004**, *27*, 601.
(3) Bish, D. L. *Bull. Mineral.* **1980**, *103*, 170.
(4) Pavan, P. C.; Gomes, G. D.; Valim, J. B. *Microporous Mesoporous Mater.* **1998**, *21*, 659.
(5) (a) Cavani, F.; Trifirò, F.; Vaccari, A. *Catal. Today* **1991**, *11*, 173. (b) McKenzie, A. L.; Fishel, C. T.; Davis, R. J. *J. Catal.* **1992**, *138*, 547. (c) Sels, B.; De Vos, D.; Buntinx, M.; Pierard, F.; Kirsch-De Mesmaeker, A.; Jacobs, P. *Nature* **1999**, *400*, 855. (d) Sels, B. F.; De Vos, D. E.; Jacobs, P. A. *Catal. Rev.* **2001**, *43*, 443. (e) Li, F.; Tan, Q.; Evans, D. G.; Duan, X. *Catal. Lett.* **2005**, *99*, 151.
(6) (a) Dékány, I.; Turi, L.; Szücs, A.; Király, Z. *Colloids Surf., A* **1998**, *141*, 405. (b) Lukashin, A. V.; Vertegel, A. A.; Eliseev, A. A.; Nikiforov, M. P.; Gornert, P.; Tretyakov, Y. D. *J. Nanopart. Res.* **2003**, *5*, 455. (c) Villegas, J. C.; Giraldo, O. H.; Laubernds, K.; Suib, S. L. *Inorg. Chem.* **2003**, *42*, 5621. (d) Nikiforov, M. P.; Chernysheva, M. V.; Eliseev, A. A.; Lukashin, A. V.; Tretyakov, Y. D.; Maksimov, Y. V.; Suzdalev, J. P.; Goernert, P. *Mater. Sci. Eng. B* **2004**, *109*, 226. (e) Gerardin, C.; Kostadinova, D.; Sanson, N.; Coq, B.; Tichit, D. *Chem. Mater.* **2005**, *17*, 6473.
(7) (a) Choy, J.-H.; Kwak, S.-Y.; Park, J.-S.; Jeong, Y.-J.; Portier, J. *J. Am. Chem. Soc.* **1999**, *121*, 1399. (b) Choy, J.-H.; Kwak, S.-Y.; Jung, Y.-J.; Park, J.-S. *Angew. Chem., Int. Ed.* **2000**, *39*, 4042. (c) Leroux, F.; Besse, J.-P. *Chem. Mater.* **2001**, *13*, 3507. (d) Darder, M.; López-Blanco, M.; Aranda, P.; Leroux, F.; Ruiz-Hitzky, E. *Chem. Mater.* **2005**, *17*, 1969. (e) Desigaux, L.; Belkacem, M. B.; Richard, P.; Cellier, J.; Léone, P.; Cario, L.; Leroux, F.; Taviot-Guého, C.; Pitard, B. *Nano Lett.* **2006**, *6*, 199.
(8) (a) Adachi-Pagano, M.; Forano, C.; Besse, J. -P. *Chem. Commun.* **2000**, 91. (b) Leroux, F.; Adachi-Pagano, M.; Intissar, M.; Chauvière, S.; Forano, C.; Besse, J. -P. *J. Mater. Chem.* **2001**, *11*, 105. (c) O'Leary, S.; O'Hare, D.; Seeley, G. *Chem. Commun.* **2002**, 1506. (d) Chen, W.; Feng, L.; Qu, B. *Chem. Mater.* **2004**, *16*, 368. (e) Jobbágy, M.; Regazzoni, A. E. *J. Colloid Interface Sci.* **2004**, *275*, 345. (f) Venugopal, B. R.; Shivakumara, C.; Rajamathi, M. *J. Colloid Interface Sci.* **2006**, *294*, 345.
(9) (a) Hibino, T.; Jones, W. *J. Mater. Chem.* **2001**, *11*, 1321. (b) Hibino, T. *Chem. Mater.* **2004**, *16*, 5482. (c) Guo, Y.; Zhang, H.; Zhao, L.; Li, G. D.; Chen, J. S.; Xu, L. *J. Solid State Chem.* **2005**, *178*, 1830. (d) Wu, Q.; Olfsen, A.; Vistad, Ø. B.; Roots, J.; Norby, P. *J. Mater. Chem.* **2005**, *15*, 4695. (e) Okamoto, K.; Sasaki, T.; Fujita, T.; Iyi, N. *J. Mater. Chem.* **2006**, *16*, 1608.
(10) (a) Li, L.; Ma, R.; Ebina, Y.; Iyi, N.; Sasaki, T. *Chem. Mater.* **2005**, *17*, 4386. (b) Liu, Z.; Ma, R.; Osada, M.; Iyi, N.; Ebina, Y.; Takada, K.; Sasaki, T. *J. Am. Chem. Soc.* **2006**, *128*, 4872. (c) Ma, R.; Liu, Z.; Li, L.; Iyi, N.; Sasaki, T. *J. Mater. Chem.* **2006**, *16*, 3803. (d) Liu, Z.; Ma, R.; Ebina, Y.; Iyi, N.; Takada, K.; Sasaki, T. *Langmuir* **2007**, *23*, 861.
(11) Li, L.; Ma, R.; Iyi, N.; Ebina, Y.; Takada, K.; Sasaki, T. *Chem. Commun.* **2006**, 3125.

highly crystalline LDHs would be particularly useful for characterizations as well as applications in ion-exchange, catalysis, and electroactive/photoactive materials, etc. Large crystals are also more desirable for obtaining well-defined LDH nanosheets upon delamination. Recently, well-crystallized Al^{3+}-based LDH crystals were made available owing to the emergence of so-called homogeneous precipitation using urea[13] or hexamethylenetetramine (HMT)[14] hydrolysis. A slow and progressive hydrolysis of urea or HMT makes the solution alkaline and induces homogeneous crystallization. The so-called homogeneous precipitation was first successfully established in Mg−Al LDH[10a,13,14] and has been readily extended to its Co−Al,[10b] Zn−Al, and Fe−Al analogs.[10d] Even ternary component M−M′−Al LDHs (M−M′: divalent Fe, Co, Ni, or Zn) have become attainable through a homogeneous precipitation of a solution containing mixed transition-metal cations and Al^{3+}.[10d] The amphoteric property of Al^{3+} plays a vital role in realizing such a homogeneous precipitation. At an initial stage during urea or HMT hydrolysis, Al^{3+} may precipitate out first as $Al(OH)_3$. As the hydrolysis progresses and the alkalinity of the solution gradually increases, the initially precipitated $Al(OH)_3$ may dissolve itself and incorporate divalent cations to form well-developed LDH host layers. The attainability of highly crystalline Al^{3+}-based LDHs through so-called homogeneous precipitation has greatly contributed to the recent success in achieving high-yield, micrometer-sized, and well-defined LDH nanosheets by a total delamination in formamide.[10]

Substituting inert Al^{3+} in the M^{3+} position for other trivalent transition-metal cations (Fe^{3+}, Co^{3+}, etc.) may bring new functionalities to LDHs. For example, the transition metals (Fe, Co) constituting LDH host slabs may function as 2D magnetic layers, if they can be delaminated. Mixed oxides, e.g., $Co_xFe_{3-x}O_4$ (also known as nonstoichiometric spinel), which is strongly magnetic, may be obtained after calcining the LDHs.[15] The calcined mixed oxides are also active as catalysts for total oxidation of carbon monoxide and hydrocarbons[15a] or as absorbents for low-temperature gas desulfurization.[15d] However, except coprecipitation, there is still no executable protocol to synthesize non-Al^{3+}-based LDHs. It has been reported that direct coprecipitation of Fe^{3+} with divalent cations (Mg^{2+}, Co^{2+}) resulted in poorly crystalline aggregates.[15,16] Though a subsequent hydrothermal treatment might improve the crystallinity to some extent,[15c] micrometer-sized monodisperse crystals have never been accomplished. Homogeneous precipitation, on the other hand, becomes somewhat impotent as transition-metal cations, unlike Al^{3+}, usually lack a desirable amphoteric feature. Obviously, new synthetic approaches to non-Al^{3+}-bearing LDHs with large crystallite sizes have to be developed.

Brucite-like phase, the simplest structure of metal hydroxides, has a close structural similarity with hydrotalcite-like LDHs. In brucite-like phase, divalent metal cations occupy octahedral sites generated by hydroxyl groups. The octahedral host layers are held together by Van der Waals' force. If a fraction of the divalent cations is replaced by trivalent cations, anions and water molecules may be incorporated into the interlayer space to balance the extra positive charge carried by trivalent cations, forming an LDH structure stabilized by electrostatic interaction between the host layers and the anions as well as by hydrogen bonds among host layer, anions, and interlayer water. As the synthesis of a brucite-like phase may not be so demanding, this structural relationship may be utilized to develop transition-metal-based LDHs. For example, it has been reported that Co^{2+} could be precipitated into highly crystalline brucite-like β-$Co(OH)_2$.[17] Though Fe^{3+} easily forms gel-like $Fe(OH)_3$ at very low pH (pH $\sim$ 2), which is a significant obstacle for the preparation of well-crystallized Fe^{3+}-bearing LDHs, Fe^{2+} may be crystallized into brucite-like $Fe(OH)_2$ at a higher pH value (pH $\sim$ 6) similar to that of Co^{2+}.[18,19] This suggests that if a brucite-like phase, e.g., $Co(OH)_2$, $Fe(OH)_2$, or $Co_xFe_{1-x}(OH)_2$ can be synthesized, a transformation into corresponding LDHs may be maneuverable through a partial oxidation of the divalent metal cations to a trivalent state.

It is known that Fe^{2+}−Fe^{3+} LDHs (green rust) may be formed as an intermediate solid when solutions containing ferrous ions are oxidized around neutrality or when iron corrodes.[19] Green rusts can also be prepared by controlling the oxidation of brucite-like $Fe(OH)_2$ in the presence of anions such as Cl^-, CO_3^{2-}, SO_4^{2-}, etc.[20] The oxidation is regarded as a topotactic reaction, but it is very fast and hence difficult to control.[21] In fact, on oxidation by air/oxygen (O_2) exposure, the transient green rust may finally transform into magnetite (Fe_3O_4), ferrihydrite (FeOOH), or maghemite (Fe_2O_3).[22] On the other hand, Fe^{3+} LDHs containing other divalent cations (Mn^{2+}, Co^{2+}) could be synthesized through an oxidation procedure similar to a mechanism of forming green rust.[23] Hansen et al. prepared $[Co^{2+}_{5.42}Fe^{3+}_{2.47}(OH)_{16}][(CO_3)_{1.12}\cdot xH_2O]$ ($x = 5-6$) by air oxidation of ferrous ions in a solution of $Co(NO_3)_2$ at pH 6.60.[23b] The product was described as spherical aggregates consisting of intergrown crystals of 0.1−0.4 μm. In addition, Xu and Zeng suggested a

(12) (a) Reichle, W. T. *Solid State Ionics* **1986**, *22*, 135. (b) Ehlsissen, K. T.; Delahaye-Vidal, A.; Genin, P.; Figlarz, M.; Willmann, P. *J. Mater. Chem.* **1993**, *3*, 883. (c) Xu, R.; Zeng, H. C. *Chem. Mater.* **2001**, *13*, 297. (d) Caravaggio, G. A.; Detellier, C.; Wronski, Z. *J. Mater. Chem.* **2001**, *11*, 912.

(13) (a) Cai, H.; Hillier, A. C.; Franklin, K. R.; Nunn, C. C.; Ward, M. D. *Science* **1994**, *266*, 1551. (b) Costantino, U.; Marmottini, F.; Nocchetti, M.; Vivani, R. *Eur. J. Inorg. Chem.* **1998**, *10*, 1439. (c) Costantino, U.; Coletti, N.; Nocchetti, M.; Aloisi, G. G.; Elisei, F.; Latterini, L. *Langmuir* **2000**, *16*, 10351. (d) Ogawa, M.; Kaiho, H. *Langmuir* **2002**, *18*, 4240. (e) Oh, J.-M.; Hwang, S.-H.; Choy, J.-H. *Solid State Ionics* **2002**, *151*, 285. (f) Adachi-Pagano, M.; Forano, C.; Besse, J.-P. *J. Mater. Chem.* **2003**, *13*, 1988. (g) Sileo, E. E.; Jobbagy, M.; Paiva-Santos, C. O.; Regazzoni, A. E. *J. Phys. Chem. B* **2005**, *109*, 10137. (h) Rao, M. M.; Reddy, B. R.; Jayalakshmi, M.; Jaya, V. S.; Sridhar, B. *Mater. Res. Bull.* **2005**, *40*, 347. (i) Kayano, M.; Ogawa, M. *Bull. Chem. Soc. Jpn.* **2006**, *79*, 1998.

(14) Iyi, N.; Matsumoto, T.; Kaneko, Y.; Kitamura, K. *Chem. Lett.* **2004**, *33*, 1122.

(15) (a) Tseung, A. C. C.; Goldstein, J. R. *J. Mater. Sci.* **1972**, *7*, 1383. (b) Fernández, J. M.; Ulibarri, M. A.; Labajos, F. M.; Rives, V. *J. Mater. Chem.* **1998**, *8*, 2507. (c) Arco, M. del; Trujillano, R.; Rives, V. *J. Mater. Chem.* **1998**, *8*, 761. (d) Baird, T.; Campbell, K. C.; Holliman, P. J.; Hoyle, R.; Noble, G.; Stirling, D.; Williams, B. P. *J. Mater. Chem.* **2003**, *13*, 2341. (e) Bernal, M. E. P.; Ruano, R. J.; Rives, V. *Ceram.—Silik.* **2004**, *48*, 145.

(16) Meng, W.; Li, F.; Evans, D. G.; Duan, X. *Mater. Res. Bull.* **2004**, *39*, 1185.

(17) Liu, Z.; Ma, R.; Osada, M.; Takada, K.; Sasaki, T. *J. Am. Chem. Soc.* **2005**, *127*, 13869.

(18) Bernal, J. D.; Dasgupta, D. R.; Mackay, A. L. *Clay Miner. Bull.* **1959**, *4*, 15.

(19) (a) Cuttler, A. H.; Man, V.; Cranshaw, T. E.; Longworth, G. A. *Clay Miner.* **1990**, *25*, 289. (b) Drissi, S. H.; Refait, Ph.; Abdelmoula, M.; Génin, J. M. R. *Corros. Sci.* **1995**, *37*, 2025. (c) Génin, J. M. R.; Bourrié, G.; Trolard, F.; Abdelmoula, M.; Jaffrezic, A.; Refait, Ph.; Maitre, V.; Humbert, B.; Herbillon, A. *Environ. Sci. Technol.* **1998**, *32*, 1058.

(20) Williams, A. G. B.; Schere, M. M. *Environ. Sci. Technol.* **2001**, *35*, 3488.

(21) (a) Lin, R.; Spicer, R. L.; Tungate, F. L.; Davis, B. H. *Colloids Surf., A* **1996**, *113*, 79. (b) Loyaux-Lawniczak, S.; Refait, Ph.; Enrhardt, J. J.; Lecomte, P.; Génin, J. M. R. *Environ. Sci. Technol.* **2000**, *34*, 438.

(22) (a) Taylor, R. M. *Clay Miner.* **1980**, *15*, 369. (b) Hansen, H. C. B. *Clay Miner.* **1989**, *24*, 663. (c) Hansen, H. C. B.; Borggaard, O. K.; Sørensen, J. *Geochim. Cosmochim. Acta.* **1994**, *58*, 2599. (d) Ona-Nguema, G.; Abdelmoula, M.; Jorand, F.; Benali, O.; Géhin, A.; Block, J. -C.; Génin, J. M. R. *Environ. Sci. Technol.* **2002**, *36*, 16.

(23) (a) Uzunova, E.; Klissurski, D.; Mitov, I.; Stefanov, P. *Chem. Mater.* **1993**, *5*, 576. (b) Hansen, H. C. B.; Koch, C. B.; Taylor, R. M. *J. Solid State Chem.* **1994**, *113*, 46.

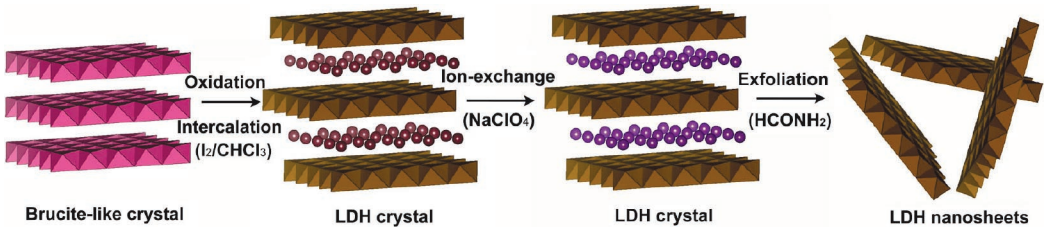

Figure 1. Schematic illustration of topochemical synthesis and exfoliation of Co^{2+}–Fe^{3+} LDHs.

possible topotactic interconversion between brucite-like and hydrotalcite-like phases in cobalt hydroxide ($Co(OH)_2$) due to redox reactions bringing a mixed valence to cobalt (Co^{2+}–Co^{3+}),[24] though the poor crystallinity of the samples made it difficult to explicitly verify the proposed topotactic nature. All these previous experimental attempts have been encouraging in verifying the feasibility of partly oxidizing divalent metal cations for the formation of an LDH phase. However, the quality of the resultant LDHs was far from satisfactory. It is clear that, in order to obtain well-crystallized transition-metal-based LDHs, an effective synthetic procedure for growing large crystals of brucite-like hydroxides and a rational method of controlling the subsequent oxidization must be explored.

Here we present an innovative topotactic approach, as a representative example, transforming brucite-like Co^{2+}–Fe^{2+} hydroxides into hydrotalcite-like Co^{2+}–Fe^{3+} LDHs. The synthetic scheme is illustrated in Figure 1. Specifically, uniformly micrometer-sized and hexagonally shaped brucite-like $Co_{2/3}Fe_{1/3}(OH)_2$ was first prepared through an HMT hydrolysis reaction. In the brucite-like bimetallic hydroxides, divalent cobalt and ferrous cations are homogeneously located in octahedral hydroxyl sheets. A unique oxidative intercalation process, by the action of iodine (I_2) in chloroform ($CHCl_3$), led to the formation of an LDH phase in which metallic cations withhold the octahedral sites in hydroxyl slabs while anions (I^-) slide into the interlayer gallery to balance the extra positive charges carried by the oxidization of Fe^{2+} into Fe^{3+}. The resultant LDHs inherited the high crystallinity from their brucite-like precursor due to the topotactic nature of the transformation. After ion-exchange into a perchlorate form, the Co^{2+}–Fe^{3+} LDHs were successfully exfoliated into unilamellar nanosheets in formamide. This is the first example of attaining highly crystalline Co^{2+}–Fe^{3+} LDHs as well as well-defined nanosheets. Topochemical transformation may now be used as a new candidate synthetic strategy, besides coprecipitation and so-called homogeneous precipitation, for creating a large family of transition-metal-based LDHs.

Experimental Section

Synthesis of Brucite-Like Co^{2+}–Fe^{2+} Hydroxides. Highly crystalline hexagonal platelets of brucite-like $Co_{2/3}Fe_{1/3}(OH)_2$ were synthesized involving the precipitation from an aqueous solution of divalent cobalt and ferrous ions through HMT hydrolysis by refluxing in a nitrogen gas atmosphere. Typically, cobalt chloride ($CoCl_2 \cdot 6H_2O$) and ferrous chloride ($FeCl_2 \cdot 4H_2O$) were dissolved in a 1000 cm^3 three-neck flask with deionized Milli-Q water to yield a total metal cation concentration of 7.5 mM ($Co^{2+}/Fe^{2+} = 2:1$). This solution was purged by a nitrogen gas flow overnight to expel air/O_2. HMT was then introduced into the solution. The mixed $CoCl_2$–$FeCl_2$–HMT solution was heated at a refluxing temperature under continuous magnetic stirring and a nitrogen gas protection. The refluxing durations were usually set at 5 h. Pink-colored solid products were recovered by quickly filtering in a glove bag filled with nitrogen gas, then washing with degassed Milli-Q water and anhydrous ethanol several times.

Topotactic Oxidative Intercalation by Iodine in Chloroform (I_2/$CHCl_3$). Theoretically, oxidizing all the ferrous cations in 1 mol of $Co_{2/3}Fe_{1/3}(OH)_2$ requires one-sixth mol of iodine. Typically, 20% excess of iodine than the required amount was dissolved in chloroform to form a purple solution. The as-prepared brucite-like $Co_{2/3}Fe_{1/3}(OH)_2$ was dispersed and magnetically stirred in the $I_2/CHCl_3$ solution at room temperature. The color of the suspension immediately changed to brown. After ~12 h, a brownish product was collected by filtering and washing with anhydrous ethanol repeatedly until the filtrate appeared colorless.

Anion-Exchange and Exfoliation of Co^{2+}–Fe^{3+} LDHs. The as-prepared brown sample, I^--intercalating LDHs, was converted into a ClO_4^- form by treating with sodium perchlorate ($NaClO_4$). (**Caution**: Sodium perchlorate is oxidative. Be careful not to mix it with organic compounds or reducing agents.) Typically, 0.5 g of the brown product was dispersed into 500 cm^3 of an aqueous solution containing 2.5 M $NaClO_4$ and 1 mM HCl. After purging with nitrogen gas, the reaction vessel was tightly capped and shaken for 1 day at room temperature. The sample was filtered, washed with water, and air-dried.

The ClO_4^- LDH (0.1 g) was mixed with 100 cm^3 of formamide in a conical beaker, which was capped air-tight after purging with nitrogen gas. Then, the mixture was ultrasonically treated for 30 min, yielding a translucent colloidal suspension. To remove possible unexfoliated particles, the resulting suspension was further treated by centrifugation at 2000 rpm for 5 min.

Characterizations. X-ray diffraction (XRD) data were recorded by a Rigaku Rint-2000 diffractometer with a monochromatic Cu Kα radiation ($\lambda = 0.15405$ nm). The morphologies and dimensions of the synthesized products were examined with a JEOL JSM-6700F field emission scanning electron microscope (FE-SEM). Transmission electron microscopy (TEM) characterizations were performed on a JEOL JEM-3100F energy-filtering (Omega type) transmission microscope equipped with an energy dispersive X-ray spectrometer (EDS) and elemental mapping/profiling capacity. A Seiko SPA 400 atomic force microscope (AFM) was used to examine the topography of the nanosheets deposited on Si wafers. A cleaned Si wafer was immersed in the colloidal formamide suspension for 5 min, which was followed by rinsing with a copious amount of water and drying under a N_2 stream. AFM images were acquired in tapping mode using a Si tip cantilever with a force constant of 20 N m^{-1}. Fourier transform infrared (FT-IR) spectra in a range of 400–4000 cm^{-1} were measured on an FTS-45RD Bio-Rad infrared spectrophotometer using the KBr pellet technique. The Co and Fe contents in the LDH samples were determined by inductively coupled plasma (ICP) atomic emission spectroscopy (Seiko SPS1700HVR) after dissolving a weighed amount of sample with an aqueous HCl solution. The I^- content was determined by ion chromatography (LC-8020) after dissolving the sample in H_2SO_4 and $Na_2S_2O_3$. The ClO_4^- was quantified from EDS measurements, correlating with chemically analyzed metallic contents. The water content was evaluated by thermogravimetry. Thermogravimetric differential thermal measurements (TG-DTA) were carried out using a Rigaku TGA-8120 instru-

(24) Xu, Z. P.; Zeng, H. C. *Chem. Mater.* **1999**, *11*, 67.

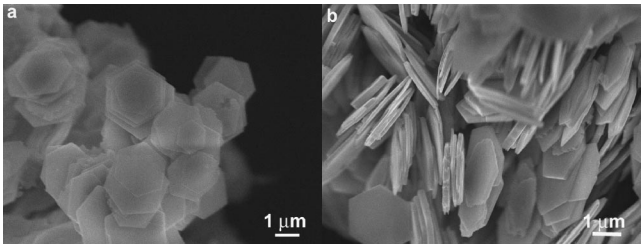

Figure 2. SEM images of as-prepared brucite-like samples.

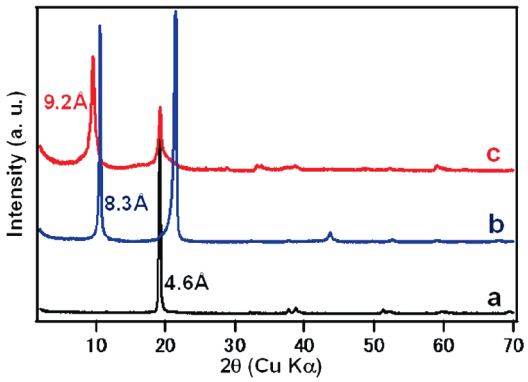

Figure 3. XRD patterns associated with the topochemical transformations: (a) as-prepared brucite-like $Co^{2+}-Fe^{2+}$ crystals, (b) $Co^{2+}-Fe^{3+}$ LDH crystals obtained by the treatment of $I_2/CHCl_3$, and (c) ClO_4^--intercalated $Co^{2+}-Fe^{3+}$ LDH crystals.

ment in a temperature range of 25−1000 °C at a heating rate of 5 °C min^{-1} under air.

Results and Discussion

Brucite-Like $Co^{2+}-Fe^{2+}$ Hydroxides. Similar to our earlier report on highly developed hexagonal platelets of β-$Co(OH)_2$,[17] refluxing the $CoCl_2-FeCl_2-HMT$ solution under N_2 atmosphere yielded pink-colored solid precipitates. The precipitates in the solution exhibited a clear anisotropic stream under stirring, implying a large aspect ratio of the product. Figure 2 shows typical SEM images of the as-prepared sample collected by filtering under N_2 protection. As can be seen, it consists of uniform hexagonal platelets with a mean lateral size of ~2 μm and a thickness of approximately ~100 nm. No impurity in other morphology was observed in the sample. A typical XRD pattern of the product is shown in Figure 3a. All the diffraction peaks can be readily indexed as a brucite-like phase with refined lattice parameters of $a = 3.198(2)$ Å and $c = 4.628(4)$ Å. The a parameter is slightly larger than that of β-$Co(OH)_2$ (3.182 Å)[17] but somewhat smaller than that of $Fe(OH)_2$ (3.258 Å, JCPDS 13-0089).[18] This might be considered to result from the different effective ionic radii of Co^{2+} (73.5 pm, high-spin) and Fe^{2+} (77.0 pm, high-spin).[25] A basal spacing of ~4.6 Å is characteristic of brucite-like phase and close to those of other brucite-like monolithic hydroxides: (β-$Co(OH)_2$, 4.658 Å; $Fe(OH)_2$, 4.605 Å). Sharp reflections in the XRD pattern reveal a high crystallinity of the sample, which is comparable to single-crystal platelets of brucite-like β-$Co(OH)_2$.[17]

The as-synthesized $Co_xFe_{1-x}(OH)_2$ presents a light pink color possibly due to the combined appearance of bimetallic contents in the hydroxides, i.e., pink β-$Co(OH)_2$ and white $Fe(OH)_2$. The ratio of metallic contents (Co/Fe) in the brucite-like product was quantified as 2.05/1.0, giving an estimated formula of $Co_{0.67}Fe_{0.33}(OH)_2$, which is consistent with the designed molar ratio of Co^{2+}/Fe^{2+} in the starting solution. For the first time, divalent cobalt and ferrous cations have been successfully coprecipitated into a single phase as brucite-like bimetallic hydroxides ($Co_xFe_{1-x}(OH)_2$) thanks to a slow and progressive precipitation induced by HMT hydrolysis. The uniform hexagonal morphology, large size, and high crystallinity of the brucite-like crystals enable a rational and precise control of the after-mentioned topotactic transformation into $Co^{2+}-Fe^{3+}$ LDHs. It is noteworthy that urea, another ammonia-releasing agent extensively utilized to synthesize highly crystalline LDHs, was not suitable for the preparation of brucite-like crystals as carbonates ions were accompanied during the urea hydrolysis. During prolonged hydrolysis of HMT, the disproportionation of formaldehyde may also produce carbonate ions, but the amount is trivial for a short reflux time, e.g., 5 h.

A careful and complete exclusion of air/O_2 from the $CoCl_2-FeCl_2-HMT$ system during the whole synthetic process as well as the filtering procedure was found to be essential to harvest pink, clean, and well-developed platelets. Otherwise, gel-like $Fe(OH)_3$ was generated due to a strong tendency of Fe^{2+} to oxidize into Fe^{3+} in the presence of oxygen in an alkaline aqueous solution. This undesirably produced gel-like $Fe(OH)_3$ precipitates adsorbed onto the $Co_xFe_{1-x}(OH)_2$ hexagonal frameworks (see the Supporting Information, Figure S1). The inclusion of $Fe(OH)_3$ imparted a miscellaneous reddish-brown color to the original pink samples. During XRD measurements, a small diffraction peak at 4.18 Å was sometimes discerned, indicating a possible dissolution of Fe^{2+} from the brucite-like sheets and oxidation by air/O_2 into FeOOH (JCPDS 81-0464) as a result of air exposure. It is therefore worth emphasizing that stoichiometric $Co^{2+}-Fe^{2+}$ hydroxides could only be obtained under the strict exclusion of air/O_2.

Topotactic Transformation into $Co^{2+}-Fe^{3+}$ LDHs. After treatment by $I_2/CHCl_3$, the pink color of the sample changed to a brownish one. As shown in Figure 3b, the basal spacing of the brownish sample was expanded to ~8.3 Å, in contrast with an initial value of ~4.6 Å for brucite-like $Co^{2+}-Fe^{2+}$ hydroxides. This indicates a possible transition to an anion-intercalated phase. The interlayer spacing, 8.3 Å, is in good agreement with the literature data on a hydrotalcite-like or LDH phase accommodating iodide ions.[26] The intensity of the first basal peak is somewhat lower than that of the second one, also implying that iodide ions with large X-ray scattering power has been intercalated between the host layers. The brown color of the transformed product suggests the existence of ferric cations. It appears that redox reactions have been involved in the phase change. The standard oxidation potential of I_2/I^- is cited as −0.535 eV, which is more oxidative than those of $Fe(OH)_3/Fe(OH)_2$, 0.58 eV, and $Co(OH)_3/Co(OH)_2$, −0.17 eV.[27] Iodine thus has a theoretical capability of oxidizing both Co^{2+} and Fe^{2+} in the brucite-like hydroxides. As a control experiment, monolithic β-$Co(OH)_2$ was also synthesized following the procedure described in our earlier paper.[17] Oxidation of the β-$Co(OH)_2$ by $I_2/CHCl_3$ was carried out under the same conditions. The

(25) Shannon, R. D.; Prewitt, C. T. *Acta Crystallogr.* **1969**, *B25*, 925.

(26) (a) Lal, M.; Howe, A. *J. Solid. State Chem.* **1981**, *39*, 368. (b) De Roy, A.; Besse, J. -P.; Bondot, P. *Mater. Res. Bull.* **1985**, *20*, 1091. (c) Iyi, N.; Fujii, K.; Okamoto, K.; Sasaki, T. *Appl. Clay Sci.* **2007**, *35*, 218.

(27) Latimer, W. M. *Oxidation Potentials*, 2nd ed.; Prentice Hall, Academic Press: New York, 1952.

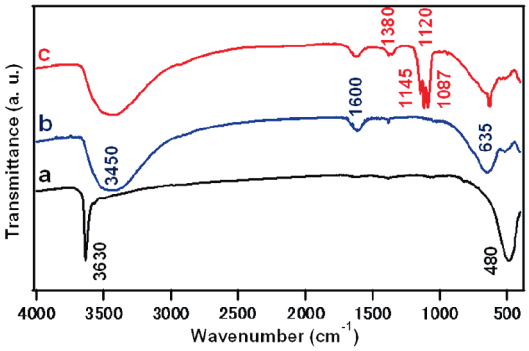

Figure 4. FT-IR spectra of (a) Co^{2+}–Fe^{2+} hydroxides, (b) I^--intercalated and (c) ClO_4^--intercalated Co^{2+}–Fe^{3+} LDHs.

result demonstrated that the oxidation of β-$Co(OH)_2$ was almost negligible (Supporting Information, Figure S2), implying that $Co(OH)_2$ may practically behave as inert due to a relatively unremarkable difference from iodine with respect to standard oxidation potentials. The transformation of Co^{2+}–Fe^{2+} hydroxides into an LDH phase may be safely considered to be the sole oxidation of Fe^{2+} to Fe^{3+} by losing electrons to I_2/I^- and simultaneous intercalation of I^-. This may be ideally expressed as the following redox reaction:

$$Co^{2+}_{0.67}Fe^{2+}_{0.33}(OH)_2 + 0.165I_2 \rightarrow Co^{2+}_{0.67}Fe^{3+}_{0.33}(OH)_2I_{0.33}$$

The refined lattice parameters of the transformed I^--intercalated Co^{2+}–Fe^{3+} LDHs are $a = 3.128(2)$ Å and $c = 24.923(4)$ Å. The a parameter is somewhat larger than that of its Co–Al analogy (3.068 Å). The expansion might be caused by a larger ionic radius of Fe^{3+} (64.5 pm, high-spin) than that of Al^{3+} (53.0 pm).[25] On the basis of the results of elemental analysis, EDS, and thermogravimetric measurements (Supporting Information, Figure S3), the chemical composition of the obtained I^--intercalated product was estimated to be $Co_{0.67}Fe_{0.33}(OH)_2I_{0.22}$-$(CO_3)_{0.055}$·$0.3H_2O$ (Anal. Calcd: Co, 30.7%; Fe, 14.4%; I, 21.7%; C, 0.5%; ignition loss, 38.6%. Found: Co, 30.7%; Fe, 14.9%; I, 21.0%; C, 0.4%; ignition loss, 38.7%). Deviating from the ideal redox reaction, a small amount of carbonate ions, possibly derived from some surface adsorbents or dissolution of CO_2 from air, might be incorporated into the oxidized phase. The water content in the formula may have originated from surface adsorbed water on precursory $Co_{0.67}Fe_{0.33}(OH)_2$ crystals or a trace amount of water impurity in the chloroform. During our experiment, commercially available chloroform (Wako Chemical Ltd., Japan), containing ~30 ppm water as read from the label, was used to dissolve iodine. This, in fact, yielded the best result for a complete phase transition to Co^{2+}–Fe^{3+} LDHs. When dehydrated chloroform was used, a mixed-layer product was instead obtained as a consequence of incomplete oxidation of Fe^{2+} and partial incorporation of anions. A new basal spacing of ~12.9 Å (Supporting Information, Figure S4) was yielded due to the alternate stacking of I^--intercalated slab (8.3 Å) and remaining brucite-like slab (4.6 Å), i.e., second staging.[26c,28] Mechanically mixing dehydrated chloroform with a small amount (e.g., 0.5 cm^3) of water was helpful to fulfill the phase change though the crystallinity of the product was significantly

(28) (a) Brindley, G. W.; Kikkawa, S. *Am. Mineral.* **1979**, *64*, 836. (b) Iyi, N.; Kurashima, K.; Fujita, T. *Chem. Mater.* **2002**, *14*, 583.

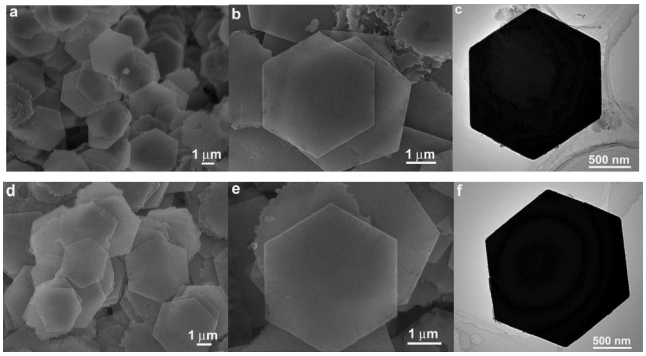

Figure 5. SEM and TEM images of Co^{2+}–Fe^{3+} LDHs accommodating iodide and perchlorate ions: (a and b) SEM images of I^--intercalated LDHs, (c) TEM image of I^--intercalated LDHs, (d and e) SEM images of ClO_4^--intercalated LDHs, and (f) TEM image of ClO_4^--intercalated LDHs.

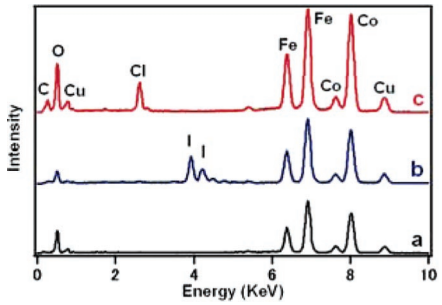

Figure 6. EDS of the transformed products in comparison with the original brucite-like Co^{2+}–Fe^{2+} hydroxides: (a) Co^{2+}–Fe^{2+} hydroxides, (b) I^--intercalated Co^{2+}–Fe^{3+} LDHs, and (c) ClO_4^--intercalated Co^{2+}–Fe^{3+} LDHs. The signals of copper (Cu) and carbon (C) originate from the carbon-coated Cu grid used to support the TEM samples.

reduced. These experimental findings reveal that a trace amount of water content is indispensable for the formation of Co^{2+}–Fe^{3+} LDHs. A hydration process incorporating water molecules into the interlayer gallery might be necessary to establish a hydrogen-bonding network among water molecules, hydroxyl slabs, and anions, which is crucial in stabilizing the LDH structure. On the other hand, attempts to achieve oxidation in aqueous solution by KI/I_2 have failed, indicating that the topotactic transformation has to be performed in an organic medium. In comparison with other organic solvents such as ethanol and acetonitrile, the oxidation performed in chloroform yielded the best results. This may be accounted for by the higher solubility of iodine in chloroform.

Ion-Exchange of Co^{2+}–Fe^{3+} LDHs. The obtained I^--intercalated Co^{2+}–Fe^{3+} LDH could be exchanged into other anionic forms by a conventional ion-exchange procedure. As shown in Figure 3c, an interlayer spacing of 9.2 Å was yielded when it was exchanged for perchlorate ions. The interlayer spacing is well consistent with the reported data of Mg–Al LDHs containing ClO_4^- (9.24 Å).[9e] The chemical composition of the ClO_4^--intercalated product was reckoned to be $Co_{0.65}Fe_{0.35}$-$(OH)_2(ClO_4)_{0.23}(CO_3)_{0.06}$·$0.45H_2O$ (Anal. Calcd: Co, 30.3%; Fe, 15.5%; C, 0.6%; ignition loss, 37.6%. Found: Co, 30.6%; Fe, 16.2%; C, 0.6%; ignition loss, 37.6%). It seems that a small amount of carbonate persists in the exchanged product. Though strict protective measures, such as carefully degassing the Milli-Q water prior to use and adding HCl to acidify the solution were taken, it was difficult to completely remove carbonate contamination. Without the addition of HCl, a full ion-exchange for a single ClO_4^--intercalated phase was hindered, represented

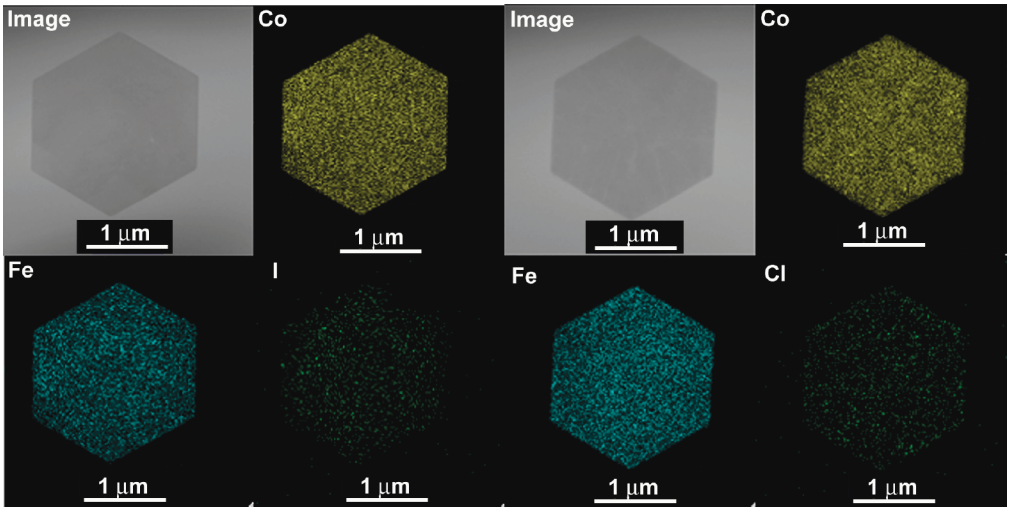

Figure 7. Elemental maps of $Co^{2+}-Fe^{3+}$ LDHs accommodating iodide ions (left panel image, Co, Fe, I maps) and perchlorate ions (right panel image, Co, Fe, Cl maps), respectively.

by a remaining shoulder peak at ~8.3 Å and even a newly emerged peak at ~7.6 Å of carbonate origin. On the other hand, a high concentration of HCl unavoidably and severely damaged the crystallinity of the exchanged product as a consequence of dissolution of metal cations from the host slabs. The optimized HCl concentration has been compromised at 1 mM to keep the carbonate content as low as possible while retaining a high crystallinity. Complemented with careful degassing, the exchanged ClO_4^--intercalated products were seemingly a single phase of 9.2 Å spacing, as shown in Figure 3c. The inclusion of carbonate ions was found to be even more severe when other anions such as NO_3^- were intended to be intercalated (Supporting Information, Figure S5). For the NO_3^- form, the basal spacing was found to be only ~7.8 Å, close to that of NO_3^--intercalated $Mg^{2+}-Fe^{3+}$ LDHs (8.04 Å) prepared by the coprecipitation method,[16] but significantly smaller than the value of ~8.8 Å typically observed for other Al^{3+} LDHs.[10] The smaller spacing may be explained by a different orientation of the intercalated nitrate ions in Fe^{3+}-based LDHs compared with that in their Al^{3+}-containing counterpart. The tilting of the NO_3^- triangular plane might be affected by the layer charge density, the total population of NO_3^- and water in the interlayer space.[26c] The tilting would be smaller for lower layer charge density. The larger size of Fe^{3+} than Al^{3+}, yielding a lower charge density, might play a role in the flat orientation of the NO_3^- triangular plane in the former but a somewhat tilted one in Al^{3+} LDHs. The reduced spacing may also be regarded as a combined consequence of the coexisting carbonate and nitrate ions due to the fact that carbonate ions, with a divalent minus charge, have a stronger affinity capable of bringing adjacent hydroxyl slabs even closer.

The above phase changes are also clearly reflected in FT-IR spectra (Figure 4). In spectrum a, $Co^{2+}-Fe^{2+}$ hydroxides show a sharp band at 3630 cm^{-1}, attributed to the OH stretching mode, which is characteristic of free OH groups in brucite-like structures. A broad absorption in the low-frequency region (centered at 480 cm^{-1}) may be assigned to M−O (M: Co/Fe) stretching and M−OH bending vibrations in the octahedral hydroxyl sheets. After treatment with $I_2/CHCl_3$ (spectrum b), a broad band centered at 3450 cm^{-1} replaces the sharp band of the OH stretching mode, which is usually interpreted as stretching modes of OH groups with hydrogen bonding and of interlayer water molecules. Another new peak at 1600 cm^{-1} is well-known as the bending mode of water molecules. Other absorptions near 600 cm^{-1} are again associated with M−O stretching and M−OH bending vibrations in the octahedral host layers. In spectrum c, besides OH and H_2O bands, new bands in the region of 1000−1200 cm^{-1} are characteristic of perchlorate ions. A weak band at 1380 cm^{-1}, due to the ν_3 mode of CO_3^{2-}, is discerned in spectra b and c, revealing a slight contamination of CO_3^{2-}.

Figure 5, parts a and b and parts d and e, displays SEM images of the transformed $Co^{2+}-Fe^{3+}$ LDHs accommodating iodide and perchlorate ions, respectively. The crystallinity of the transformed products, in terms of size, shape, and morphology, was essentially the same as that of the initial $Co^{2+}-Fe^{2+}$ hydroxides crystals. It thus confirms the topotactic feature that the crystallinity of the brucite-like precursory platelets was perfectly retained during the subsequent redox and ion-exchange processes. This is also evidenced by the intact hexagonal morphology shown in TEM observations (Figure 5, parts c and f)). Figure 6 displays typical EDS spectra taken from individual platelets, revealing the incorporation of iodide ions during the redox reaction and perchlorate ions (represented by chlorine and oxygen) during the ion-exchange process. Employing a sophisticated microscopic technique of elemental mapping, it is further possible to identify the spatial elemental distribution of the platelets. Figure 7 shows the elemental maps of $Co^{2+}-Fe^{3+}$ LDHs accommodating iodide (left panel) and perchlorate ions (right panel), respectively. It is apparent that Co and Fe are homogeneously distributed in each individual platelet. These microscopic and spectroscopic evidence clearly demonstrated two important aspects of the present synthetic approach: (1) the as-synthesized and evolved products are indeed bimetallic $Co^{2+}-Fe^{2+}$ and $Co^{2+}-Fe^{3+}$ hydroxides, not separated $Co(OH)_2$/$Fe(OH)_2$ or monolithic hydroxides with mixed valences (e.g., $Co^{2+}-Co^{3+}$, $Fe^{2+}-Fe^{3+}$); (2) the transformations are of genuine topotactic nature with excellent maintenance of shape, size, and crystallinity.

Exfoliation. Through ultrasonically dispersing ClO_4^- LDHs in formamide, a translucent colloidal solution of brown color was yielded, suggesting the occurrence of delamination. The

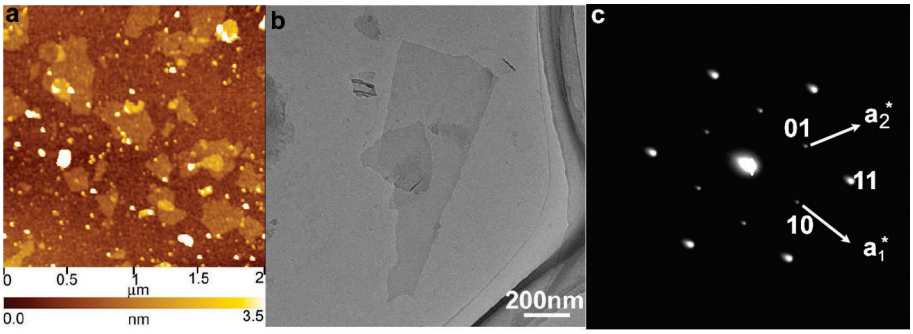

Figure 8. $Co^{2+}-Fe^{3+}$ LDH nanosheets: (a) AFM observation, (b) TEM image, and (c) SAED pattern taken from an individual nanosheet.

morphology and size of the exfoliated nanosheets were examined by AFM and TEM. A tapping-mode AFM image in Figure 8a shows sheets with ultimate thin thickness and lateral dimensions of a few hundreds of nanometers on the Si wafer. Some nanoparticles of a few nanometers are also observed. They are speculated to be some carbonate-originated unexfoliated particles, unable to be removed by centrifugation due to their tiny dimensions. The ultrathin nanosheets are somewhat irregular in shape, indicating possible severe breakage or fracture of the parent ClO_4^- LDHs hexagonal crystallites during the delamination process. The height profile of the nanosheets reveals an average thickness of ~0.8 nm. This value is very similar to those previously observed for Mg−Al, Co−Al, and other ternary LDH nanosheets.[10] Such a thickness undoubtedly demonstrates the unilamellar nature of the nanosheets. A typical TEM image (Figure 8b) also visualizes some sheetlike objects of irregular shapes. The sheets exhibit very faint but homogeneous contrast, reflecting their ultrathin and uniform thickness. The lateral dimension, a few hundreds of nanometers, also agrees well with that identified by AFM observations. As shown in Figure 8c, the selected area electron diffraction (SAED) pattern taken from an individual sheet displays hexagonally arranged spots with a lattice constant of $a = 3.1$ Å, compatible with the in-plane unit cell of parent LDH crystals. This offers strong evidence that the intralayer architecture of the LDHs remains unchanged during the exfoliation.

Mechanical shaking could not achieve the delamination of $Co^{2+}-Fe^{3+}$ LDHs, regardless of what the anionic species (I^-, ClO_4^-, NO_3^-) are. This is different from previous reports on delamination of Al^{3+} LDH in formamide, where mechanical shaking was usually required.[10] Ultrasonically treating other anionic forms of $Co^{2+}-Fe^{3+}$ LDHs (I^-, NO_3^-) did not yield an obvious delamination, either. The reason is not clear yet, but we suspect it may be either ascribed to the aforementioned different anion affinity inherent with different LDHs, which may strongly affect the delamination ability, or the small amount of miscellaneous carbonate ions in the present $Co^{2+}-Fe^{3+}$ LDHs. A systematic study may be carried out in the future to understand the general rules governing the delamination behavior of different LDHs intercalated with different counter anions.

Conclusion

An innovative topotactic approach has been performed to successfully prepare highly crystalline hexagonal platelets of $Co^{2+}-Fe^{3+}$ LDHs from precursory brucite-like $Co^{2+}-Fe^{2+}$ hydroxides. An oxidative intercalation process, employing iodine dissolved in chloroform, was a key process in realizing such a topotactic evolution. Abundant microscopic and spectroscopic facts provided compelling evidence for the topotactic nature of the transformation. This is the first example of synthesizing highly crystalline non-Al^{3+} and transition-metal-based LDHs. Furthermore, $Co^{2+}-Fe^{3+}$ LDHs intercalated with perchlorate anions could be exfoliated into unilamellar nanosheets in formamide by ultrasonic treatment. $Co^{2+}-Fe^{3+}$ LDHs nanosheets are promising for magnetic property investigations in a true 2D system. They may also be used as building blocks for thin film devices and core/shell composite structures. The topochemical principle might be easily extended to prepare $Co^{2+}-Fe^{3+}$ LDHs in various Co/Fe ratios, or more important, to other series of transition-metal-based LDHs such as $Ni^{2+}-Fe^{3+}$, $Co^{2+}-Co^{3+}$, etc.

Acknowledgment. This study was supported by CREST of the Japan Science and Technology Agency (JST).

Note Added after ASAP Publication. Due to a production error, the wrong image was used as Figure 6 in the version of this paper published on March 30, 2007. The figure was replaced with the correct version on April 3, 2007.

Supporting Information Available: SEM images of brucite-like $Co^{2+}-Fe^{2+}$ crystals contaminated with $Fe(OH)_3$, XRD pattern of β-$Co(OH)_2$ treated by $I_2/CHCl_3$, thermogravimetric data, I^--intercalated products obtained by treating $Co^{2+}-Fe^{2+}$ hydroxides in different solvents, FT-IR spectrum and XRD pattern of NO_3^--intercalated $Co^{2+}-Fe^{3+}$ LDHs. This material is available free of charge via the Internet at http://pubs.acs.org.

JA0693035